Vol. 50 · No. 11
ISSN 0091-3286 | November 2011

Optical Engineering

SPIEDigitalLibrary.org/oe

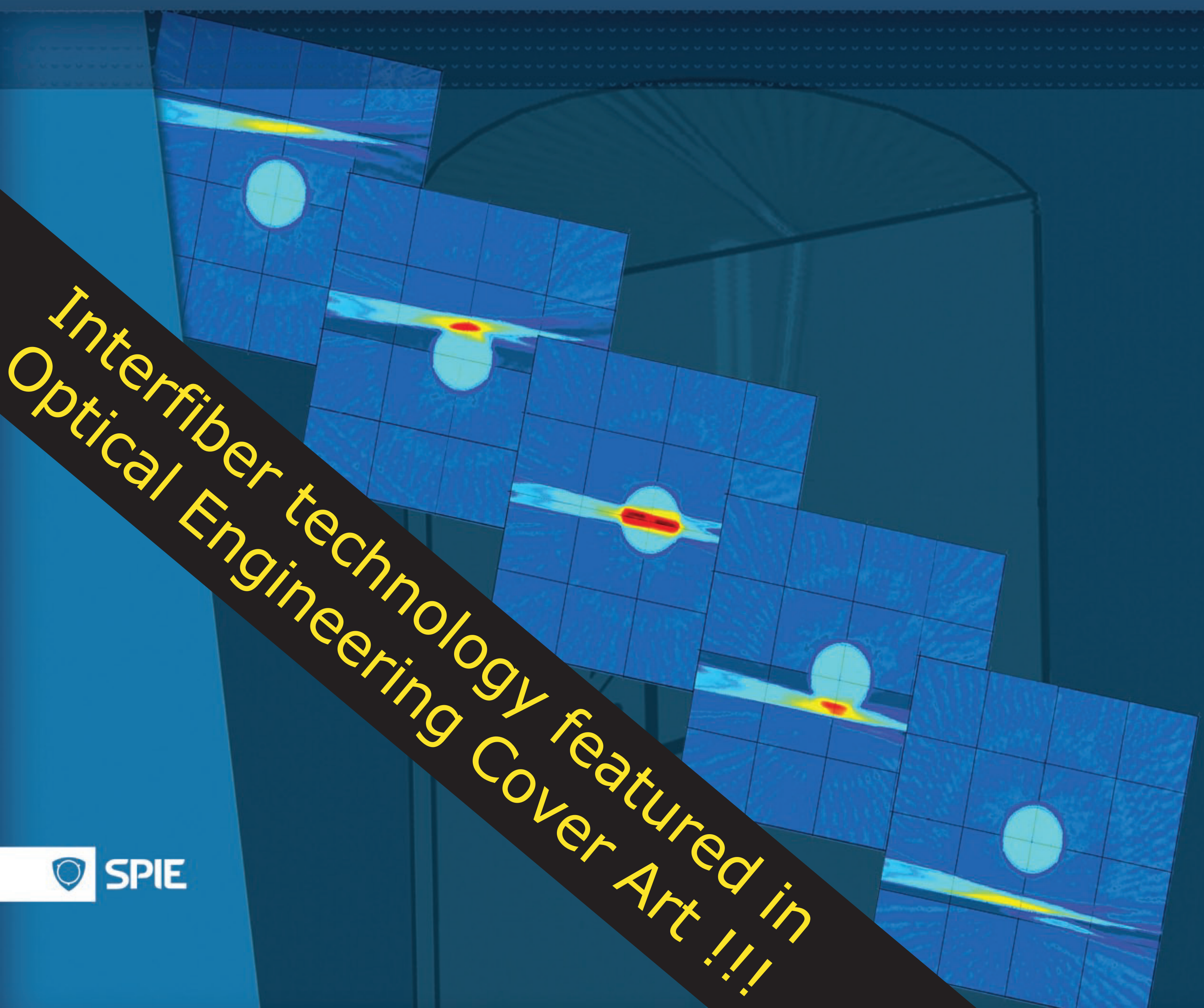

SPIE

New transverse techniques for characterizing high-power optical fibers

Andrew D. Yablon
Interfiber Analysis
26 Ridgewood Drive
Livingston, New Jersey 07039
E-mail: andrew_yablon@interfiberanalysis.com

Abstract. Novel transverse techniques for measuring the refractive index profile and spontaneous emission of high-power optical fibers are described. These techniques are particularly attractive for measuring fiber samples incorporating axial variations, such as mode transformers, gratings, fusion splices, tapers, taps, or couplers. Computerized tomography of spontaneous emission is demonstrated as the first nondestructive method for estimating the spatial distribution of gain in a rare earth–doped fiber, which can be particularly useful when exploiting a spatially inhomogeneous dopant profile. [DOI: 10.1117/1.3609812]

Subject terms: optical fiber measurements; refractive index measurements; rare earth–doped optical fibers; high-power optical fibers; computerized tomography; fiber characterization.

Paper 110270SSPR received Mar. 19, 2011; revised manuscript received Jun. 13, 2011; accepted for publication Jun. 20, 2011; published online Sep. 30, 2011.

1 Introduction

For the past 15 years, the maximum output power of rare earth–doped optical fiber lasers and amplifiers has been growing at the remarkable rate of ~2 dB/yr.[1] This remarkable growth is partly due to novel fiber designs, fiber-based components, and innovative fiber manufacturing techniques that in turn, benefit from fiber measurement and characterization technologies. In this paper, we discuss two new transverse approaches for characterizing high-power optical fibers and fiber-based components: multiwavelength interferometry (MWI) and computerized tomographic imaging of spontaneous emission (SE) from rare earth–doped fibers. These new measurement techniques will contribute to the design and fabrication of new high-power optical fibers and fiber-based components.

Although powerful approaches exist for characterizing both the refractive index and gain dopant distribution of optical fiber performs,[2] characterization techniques for drawn fibers remains critically important because (*i*) many high-power fibers are assembled by a stack-and-draw method on a draw tower and, therefore, no preform is available for measurement; (*ii*) manufacturers of high-power optical fibers typically do not share proprietary preform measurements with their customers; and (*iii*) the fiber draw process has been shown to strongly affect the properties of the resulting fiber.[2,3]

The effectiveness of high-power optical fibers depends primarily on the transverse distribution of refractive index in the fiber, often termed the refractive index profile (RIP). The RIP determines the transverse spatial distribution of any guided modes as well as their response to external perturbations such as coiling. Early fiber designs (both single- and multimode) were simple step-index structures comprised of only a single core surrounded by a lower index cladding. Contemporary fiber designs exploit complex structures, often including annular trenches and rings, and even nonazimuthally symmetric RIPs, to achieve desired performance. Material dispersion is known to affect the RIP, manifesting itself as a spectral dependence that can be quantified with multiwavelength interferometry.[4,5]

In an analogous fashion, the amplifying properties of a rare earth–doped optical fiber are affected by the transverse distribution of rare-earth dopant and its host glass composition, which can be termed the spontaneous emission profile (SEP). In parallel to early passive fibers, early telecom fiber amplifiers consisted of a step-index rare earth–doped core amplifying a single guided mode. Recently, far more complex rare earth–doped fiber designs have been proposed, including designs in which the rare-earth dopant is confined inside the center of the core,[6–13] in a ring outside of the core,[14,15] or as part of a complex higher-order mode waveguide.[16] These new fiber designs demand new techniques for measuring a fiber's transverse gain distribution, or SEP.

In addition to fiber designs that exhibit complex transverse profiles, high-power fiber sources and amplifiers typically incorporate various fiber-based devices such as mode transformers, pump combiners, couplers, gratings, physical tapers, taps, and fusion splices. The RIP or SEP of such axially inhomogeneous fiber-based components can only be assessed by techniques that operate transversely through the side of the fiber. For this reason, most new fiber characterization techniques, including the ones described here, are based on transverse arrangements[17–20] that can optically section the fiber sample. One disadvantage of transverse fiber characterization is the need to utilize some type of computerized tomography when the sample is not azimuthally symmetric. Fortunately, computerized tomographic technologies originally developed for medical applications have been applied to the problem of optical fiber characterization.[21,22] Because the measurement techniques described here do not require access to the end of the fiber under test (FUT), they could even be performed on a live fiber carrying an optical signal, although the removal of the coating and immersion in oil would pose difficulties for cladding pumped fibers.

0091-3286/2011/$25.00 © 2011 SPIE

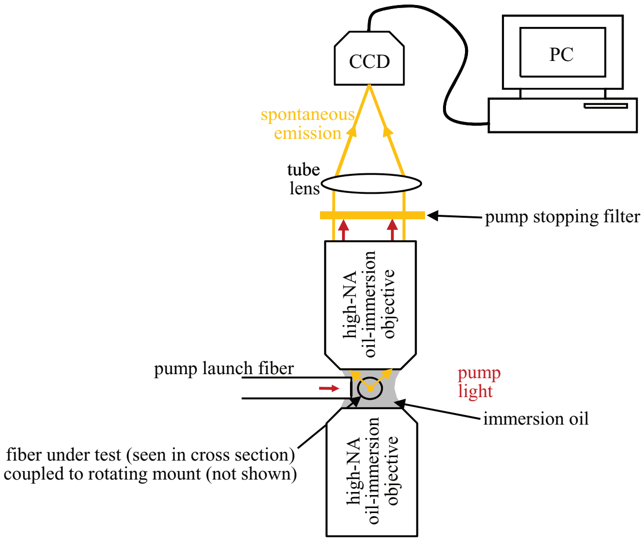

Fig. 1 Schematic illustration of experimental apparatus used to measure the SEP of optical fiber samples. Note that the lower oil-immersion objective lens serves as a mechanical substrate for the immersion oil and does not participate in the measurement.

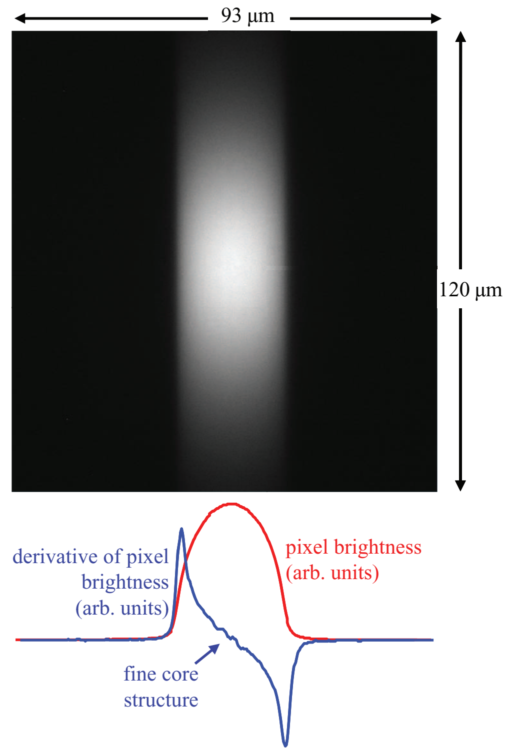

Fig. 2 Sample SEP intensity image showing the SE from the 25-μm-diam core of the FUT (Thorlabs Yb1200–25/250DC). The FUT is oriented vertically in this image and the field width (93 μm) is much less than the fiber diameter so that the fiber's cladding edges lie outside the field of view. The brightness gradient in the vertical direction is due to the finite spot size of the pump radiation.

2 Experimental Methods

The experimental apparatus used for MWI has been previously described.[4,5] Data were obtained on high-power rare earth–doped optical fibers by combining this approach with computerized tomography.[4,21,22] Unlike the approach advocated by Bachim *et al.*,[22] phase data were acquired at every 5 deg over only 175 deg (36 total scans), which significantly accelerated data acquisition and processing time. Furthermore, axial sections of fiber only 1.5 μm long were analyzed by restricting the data analysis to eight rows of the CCD camera in which each CCD row corresponded to $\sim$0.185 μm of axial fiber length.

A diagram of the experimental apparatus employed for SEP measurement is shown in Fig. 1.[23] The FUT is positioned in the focal plane of an infinity-corrected oil-immersion microscope objective and pumped transversely, rather than axially. The cleaved end of a single-mode pump launch fiber is inserted into the meniscus of immersion oil and launches continuous-wave pump laser light ($\sim$130 mW at 976 nm from a QPhotonics fiber-coupled laser diode) from the side. Because the pump launch fiber is mounted on a three-axis translation stage its position is optimized based on the intensity of the detected SE. The optimum distance between the pump launch fiber tip and the FUT was found to be $\sim$1 mm, and because the pump launch fiber's mode field diameter is $\sim$7 μm, it casts an $\sim$100-μm-diam Gaussian spot on the core of the fiber under test (Fig. 2). The single-mode fiber source emits a spatially coherent spherical wave in its far field that ensures the pumping is spatially homogeneous. In principle, graded-index fiber lens tipped fibers[24] could be used to provide a larger, more planar pumping, although that was not implemented for the experiments described here. Typical rare-earth core diameters are between 5 and 50 μm in diameter, and therefore, the pump energy is negligibly depleted when traversing such microscopic distances, again ensuring spatial homogeneity of the pump source.

The refractive index oil ensures that the reflectance experienced by the laser pump is negligible and that the cladding surface of the FUT does not refract either the pump or SE signals. Furthermore, the refractive index oil permits the objective lenses to achieve extremely high numerical aperture thereby achieving submicron spatial resolution. The pump light excites any rare-earth dopants (i.e., Yb) present in the FUT thereby producing SE. The SE is captured by the high–numerical aperture (NA) infinity-corrected oil-immersion objective lens and imaged onto the active area of a conventional 16-bit-depth silicon CCD camera by a tube lens. Although such silicon CCD cameras are only weakly sensitive in the near-infrared, they are adequate for this application. As for most other transverse fiber interrogation techniques,[17] the fiber's polymer coating is turbid and must be removed to provide micron-scale spatial resolution so that the cladding glass is in contact with the surrounding refractive index oil.

MWI is a phase-based method to measure a fiber's RIP and therefore depends on temporal and spatial coherence between the probe light traversing the fiber sample and the reference light in a reference beam.[4,5] By contrast, the spontaneous emission collected from the optically pumped section of the rare earth–doped core is both spatially and temporally incoherent. This poses no difficulty because tomographic reconstruction based on this spontaneous emission is a pure amplitude phenomenon and therefore does not require coherence.

Two aspects of the experimental setup preclude the possibility that the CCD measures spurious pump signal

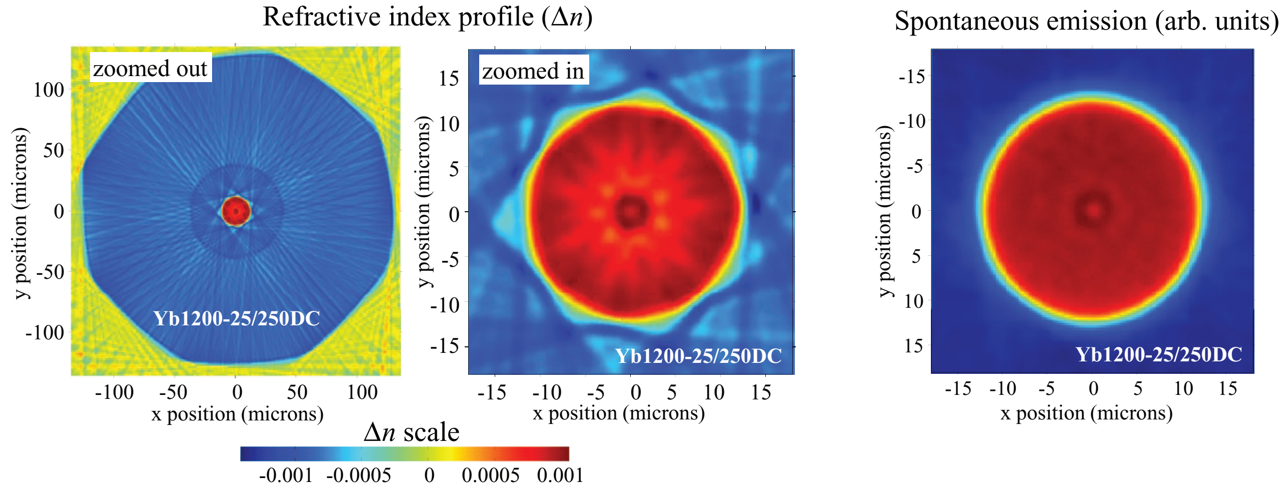

Fig. 3 Refractive index profile (zoomed out at left and zoomed in middle plot) was measured at 955 nm. The false color of the refractive index profile is indicted by the color legend below the index profile maps. The spontaneous emission profile (right) is also shown in false color, but with arbitrary units. (Color online only.)

power: (*i*) a 90-deg angle between the pump signal axis and the CCD imaging axis, and (*ii*) a pump-stopping filter placed between the objective and the tube lens. The pump-stopping filter was a long-pass optical interference filter (Thorlabs FEL1000) cutting on at 1000 nm. The efficacy of this filter was verified by comparing its optical density (OD) when pumping a Yb-doped FUT, as shown in Fig. 1 (OD $\approx$ 0.92 or 12% power transmission) to its optical density (OD) when it was shielding the CCD camera from direct illumination by the laser diode pump (OD $\approx$ 3.3 or 0.05% power transmission). The profound difference in filter attenuation shows that the signal emitted by the FUT does not have the same spectral content as the laser diode pump and therefore must not be elastically scattered by the FUT. Although the pump was known to have a wavelength of 976 nm, the SE is presumed to be distributed over the range of $\sim$980 to $\sim$1100 nm, as is typical for Yb-doped high-power optical fibers.

A desktop PC acquires and processes the intensity images detected by the CCD camera. Figure 2 shows a typical intensity image acquired on a commercially available double-clad large-mode-area high-power Yb-doped fiber (Thorlabs Yb1200–25/250DC) with a 25-μm-diam core and a 250-μm-diam octagonal cladding using the setup depicted in Fig. 1. The FUT is oriented vertically, and the bright region in the center of the image is the core of the FUT. The variation in brightness in the vertical direction results from the finite spot size of the pump radiation. The variation of brightness with lateral position is quantified from the 16-bit-depth CCD image. Several rows of pixels are extracted from the center of the image in Fig. 2 (green line) where the pump illumination is strongest and these brightness values are depicted below the image (red trace, arb. units). The derivative (blue trace) of the brightness values highlights fine features that correspond to authentic fine structure in the fiber's core. As for RIP measurement using multiwavelength interferometry, the FUT was rotated about its axis through a total range of 175 deg using a fiber rotation chuck (not shown in Fig. 1) and data were acquired every 5 deg. An inverse Radon transform converted the collection of transverse brightness traces into a two-dimensional SEP.

3 Results

In Fig. 3, the SEP from the 25-μm core fiber is compared to its two-dimensional RIP measured by multiwavelength interferometry at 955 nm. The rotational orientation of the fiber is identical in both measurements; although, the fiber's core appears to be substantially axisymmetric. The octagonal cladding of the fiber is evident in the zoomed out fiber index profile. The region outside of the fiber is refractive index matching oil, nominally $\sim$1.451 at 955 nm. It is worth noting that the refractive index contrast shown in Fig. 3 is very small; the total range of the false color is $\sim$0.0025, and the core-to-clad numerical aperture is only $\sim$0.07. Weak fanlike artifacts are evident at large radius in the refractive index profile due to the relatively large 5-deg interval between tomographic projections and also because of the octagonal cladding surface. The SE profile does not exhibit these artifacts because the cladding surface does not interact with the pump or SE signal. An $\sim$3μmdiam circular ridge (corresponding to the ripples in the blue trace of Fig. 2) is evident in the center of the core in both the refractive index and SE measurements, which strongly suggests that it this is a real feature. Furthermore, this fine feature demonstrates the submicron resolution of both measurement techniques.

To further compare the fiber index profile to the SE, the data shown in Fig. 3 were averaged over all azimuthal angles to produce the traces shown in Fig. 4. This averaging eliminates the fanlike artifacts from the fiber index profile and suppresses noise thereby permitting a high-quality comparison between the two measurements. Although both traces show a similar ripple near the center of the core and substantially agree concerning the fiber's core dimension, the index profile shows a trench at a radius of $\sim$4 μm that is absent from the SE profile.

Figure 5 compares the SEP obtained from two different double-clad large-mode-area Yb-doped fibers (Thorlabs Yb1200–25/250DC and Thorlabs Yb1200–20/400DC) and further demonstrates the possibilities of this new fiber measurement approach. Not surprisingly, the core diameter of the Yb1200–20/400DC evident from its SEP agrees with the expected 20 μm. Both the two-dimensional SEP and the azimuthally averaged data [Fig. 5(b)] show subtle differences

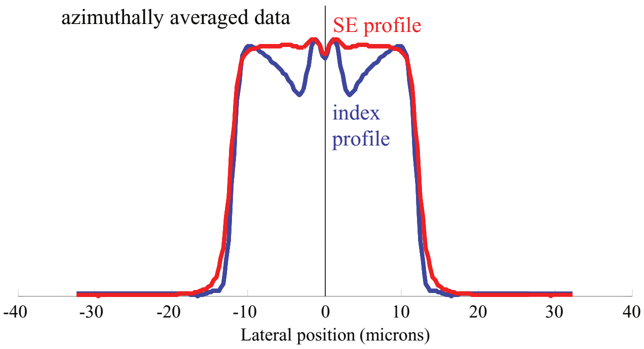

Fig. 4 Azimuthally averaged comparison between fiber index profile (red trace, normalized units) and SE profile (blue trace, normalized units) obtained for 25-μm-diam core 250-μm-diam cladding fiber. Although there is strong agreement concerning the core diameter and the ripple in the core's center, the index profile shows a trench with a radius of $\sim$4 μm. (Color online only.)

in the core structure. More significantly, the intensity of each SEP is slightly different, perhaps indicating a slight difference in Yb concentration, or perhaps differences in the host glass.

Figure 6 demonstrates how multiwavelength interferometry can be used to probe fusion splices[18,25] and mode transformers. A sample of Thorlabs GF1AA fiber was fusion spliced to another fiber, and refractive index profiles were taken at $\sim$100-μm intervals in the vicinity of the fusion splice. Refractive index perturbations associated with dopant diffusion and cladding refractive index changes are evident in the traces. The spatial distribution of the guided modes traversing this region can be modeled based on these RIP measurements.

Aside from fusion splices, another type of axially inhomogeneous fiber-based device is an inline optical tap or coupler. Such devices can be constructed using the traditional fused fiber approach, or alternatively with the aid of a femtosecond laser.[26] Figure 7 shows the 2-D tomographic refractive index profile of a waveguide written by a femtosecond laser at an angle to the core of a single-mode fiber. Such a waveguide provides the functionality of a low-loss wavelength-insensitive inline optical power tap by diverting a small fraction of the propagating signal out of the core to a location where it can be measured.[26]

4 Discussion

It is important to understand that signal amplification in a rare earth–doped fiber depends on the host glass composition as well as the rare-earth dopant distribution. The technique described here measures the distribution of spontaneous emission in a homogeneously pumped fiber sample and therefore cannot distinguish between a favorable host glass and an unfavorable rare-earth doping concentration or vice versa. Although these issues may vex the fiber manufacturer, they are typically of secondary concern to the fiber consumer, who is typically interested in the spatial distribution of gain. It is also worth noting that the spatial distribution of gain in a rare earth–doped fiber also depends on the spatial distribution of pump light, which is not considered in the measurement technique described here.

In principle, the RIP and SEP could be measured in the manner described here on an experimental apparatus incorporating both techniques. Although the veracity of the discrepancy between the RIP and the SEP found inside the core of Yb1200–25/250DC in Fig. 4 cannot be independently verified, this discrepancy highlights the fact that the refractive index profile is not always a valid surrogate for the rare-earth dopant distribution. Discrepancies between the dopant concentration in the preform and the refractive index in the preform have been observed before.[3] Furthermore, the multiplicity of dopants comprising the fiber's core may not contribute to the refractive index in an additive manner, particularly when both aluminum and phosphorus are present.[3]

When the total cladding pump absorption is known, the spatially resolved pump absorption can be computed based on the measured SEP. For example, an estimate of the linear absorption coefficient of the pump inside the core can be made for the fibers plotted in Fig. 5 based on their core/clad area ratios and the manufacturer specified total cladding pump absorptions. The total cladding pump absorptions for Yb1200 25/250DC and Yb1200 20/400DC are specified as 2.5 dB/m and 0.7 dB/m, respectively. The core/clad area ratios for Yb1200 25/250DC and Yb1200 20/400DC are about 0.01 and 0.0025, respectively. Assuming that the cladding modes are uniformly populated by pump energy, the linear

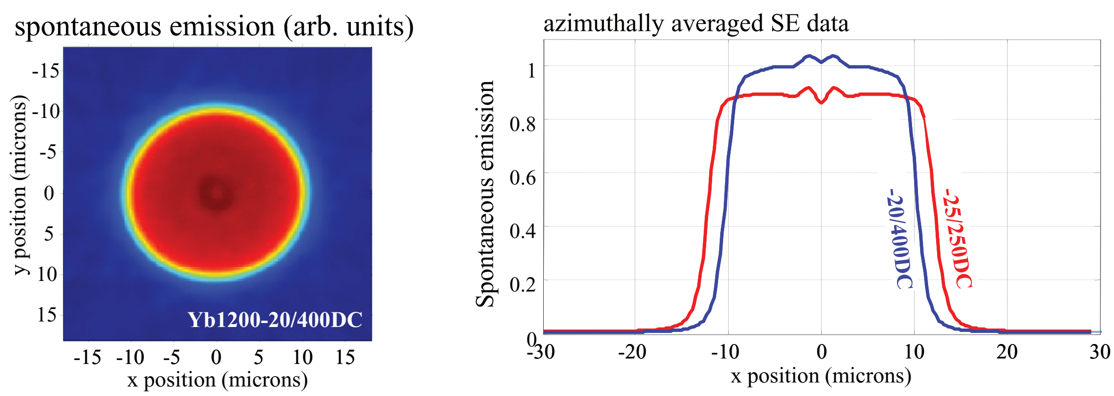

Fig. 5 Two-dimensional spontaneous emission profile obtained from Thorlabs Yb1200–20/400DC fiber (left) and comparison between azimuthally averaged data obtained from Thorlabs Yb1200–20/400DC fiber and Thorlabs Yb1200 25/250DC fiber (right). The *y*-axis units on the right hand plot are arbitrary but the relative difference in SE intensity is real.

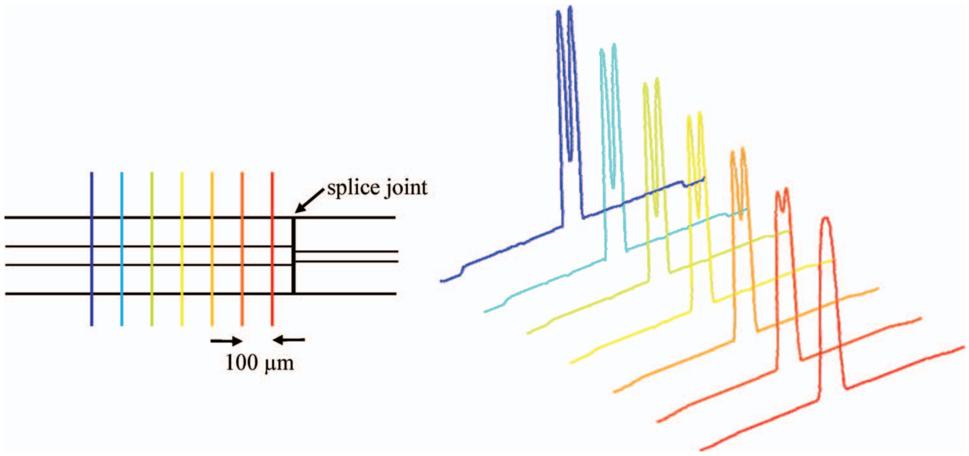

Fig. 6 Optical sections taken through a fusion splice of Thorlabs GF1AA optical fiber using multiwavelength interferometry. Diffusion of the core dopant is evident in the region adjacent to the fusion splice while other more subtle changes to the fiber's cladding are evident as well.

absorption coefficients of the pump in the core are predicted to be ~5.18/m (22.5 dB/m) and ~6.15/m (26.71 dB/m) for Yb1200 25/250DC and Yb1200 20/400DC, respectively. In other words, the predicted ratio in the linear absorption coefficients of the pump in the core is ~1.18, whereas the measured ratio between the SE intensity in Fig. 5 is ~1.13, which is good agreement considering the assumptions required for the calculation. This type of analysis points the way towards determining a spatially resolved linear absorption coefficient based on the SEP intensity profile and the total measured cladding pump absorption coefficient. The spatially resolved pump absorption could conceivably be used to accurately predict the modal gain dynamics of a rare-earth fiber in a high-power laser or amplifier.[27] Such modal gain dynamics are critical for achieving excellent beam quality in a multimode fiber design.

Photodarkening is a poorly understood but serious impediment to the performance of many rare earth–doped fiber

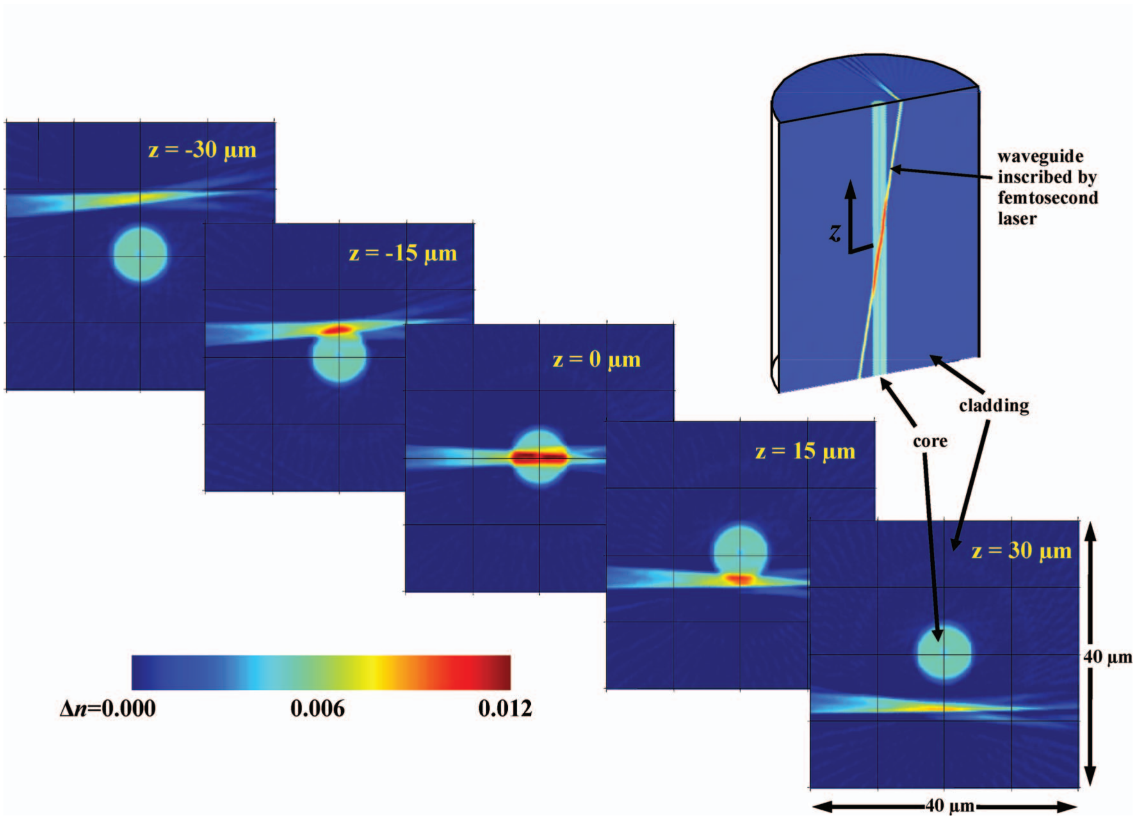

Fig. 7 False color optically sectioned RIP of single-mode fiber core and refractive index perturbation inscribed by a femtosecond laser. Each frame was acquired via multiwavelength interferometry combined with computerized tomography of 36 projections taken every 5 deg from 0 to 175 deg. Inside each image, the boxes are 10 μm on each side so the total domain depicted by each image is the central 40 $\times$ 40 μm region of the fiber. Each optical section represents data integrated over an axial length of only ~1.5 μm at distinct axial (z) positions. The refractive index perturbation inscribed by the femtosecond laser is seen to be about +0.007 inside both the core and cladding of the fiber. (Color online only.)

lasers and amplifiers.[1] Recent investigations[28] have provided evidence that photodarkening in Yb fibers is not spatially homogeneous but instead varies transversely depending on the fiber design and optical energy distribution. Near-field intensity profiles were used[28] to indirectly infer the spatial dependence of photodarkening. The SEP technique described here may offer a more direct measurement of spatially resolved photodarkening in Yb-doped fibers.

Although these results were obtained for conventional Yb-doped silica fibers, this technique can also be applied to Er, Bi, Tm, or other dopants, and this technique can also be applied to nonsilica optical fibers. Of course, the detector and imaging optics must be effective in a spontaneous emission band.

5 Conclusions

Continued advances in the development of high-power optical fibers will depend on new approaches for characterizing such fibers. To this end, we have described new nondestructive computerized-tomography techniques capable of measuring the RIP and SEP of high-power optical fibers. We applied these techniques to commercially available double-clad rare earth–doped large-mode-area high-power optical fibers and found small, but intriguing, differences between the RIP and SEP. Knowledge of the cladding pump absorption coefficient permits computation of the spatially resolved pump absorption coefficient, which could be a powerful tool for predicting modal dynamics in high-power fibers. The application of the new transverse fiber characterization techniques to measuring axially inhomogeneous fiber samples, such as a fusion splice and an optical fiber power tap, was demonstrated. Other applications could include mode converters, physical tapers, gratings, or couplers. This technique could also be applied to a variety of rare-earth dopants and also to nonsilica optical fibers.

Acknowledgments

The author thanks OZ Optics for graciously providing the optical fiber tap depicted in Fig. 7 and Chiral Photonics for kindly loaning the laser diode used for the SEP measurements.

References

1. D. J. Richardson, J. Nilsson, and W. A. Clarkson, "High power fiber lasers: current status and future perspectives," *J. Opt. Soc. Am. B* **27**(11), B63–B92 (2010).
2. J. Kirchhof, S. Unger, A. Schwuchow, S. Jetschke, and B. Knappe, "Spatial distribution effects and laser efficiency in Er/Yb doped fibers," *Proc. SPIE* **5350**, 222–233 (2004).
3. S. Unger, A. Schwuchow, J. Dellith, and J. Kirchhof, "Codoped materials for high power fiber lasers – diffusion behavior and optical properties," *Proc. SPIE* **6469**, 646913 (2007).
4. A. D. Yablon, "Multiwavelength optical fiber refractive index profiling," *Proc. SPIE* **7580**, 758015 (2010).
5. A. D. Yablon, "Multi-wavelength optical fiber refractive index profiling by spatially resolved fourier transform spectroscopy," *J. Lightwave Technol.* **28**(4), 360–364 (2010).
6. H. L. Offerhaus, N. G. Broderick, D. J. Richardson, R. Sammut, J. Caplen, and L. Dong, "High-energy single-transverse-mode Q-switched fiber laser based on a multimode large-mode-area erbium-doped fiber," *Opt. Lett.* **23**(21), 1683–1685 (1998).
7. J. M. Sousa and O. G. Okhotnikov, "Multimode Er-doped fiber for single-transverse-mode amplification," *Appl. Phys. Lett.* **74**(11), 1528–1530 (1999).
8. N. G. Broderick, H. L. Offerhaus, D. J. Richardson, R. Sammut, J. Caplen, and L. Dong, "Large mode area fibers for high power applications," *Opt. Fiber Technol.* **5**, 185–196 (1999).
9. J. R. Marciante, R. G. Roides, V. V. Shkunov, and D. A. Rockwell, "Near-diffraction-limited operation of step-index large-mode-area fiber lasers via gain filtering," *Opt. Lett.* **35**(11), 1828–1830 (2010).
10. J. M. Oh, C. Headley, M. J. Andrejco, A. D. Yablon, and D. J. DiGiovanni, "Increased amplifier efficiency by matching the area of the doped fiber region with the fundamental fiber mode," in *Proc. of Optical Fiber Commun. Conf.* (OFC) 2005, Anaheim, Paper No. OThC6 (2005).
11. J. M. Oh, C. Headley, M. J. Andrejco, A. D. Yablon, and D. J. DiGiovanni, "Increased pulsed amplifier efficiency by manipulating the fiber dopant distribution," presented at Conf. on Lasers and Electro-Optics 2006, Long Beach, CA, Paper No. CTuQ3 (2006).
12. T. Kokki, J. Koponen, M. Laurila, and C. Ye, "Fiber amplifier utilizing an Yb-doped large-mode-area fiber with confined doping and tailored refractive index profile," *Proc. SPIE* **7580**, 758016 (2010).
13. M. Hotoleanu, M. Söderlund, D. Kliner, J. Koplow, S. Tammela, and V. Philipov, "High order modes suppression in large mode area active fibers by controlling the radial distribution of the rare earth dopant," *Proc. SPIE* **6102**, 61021T (2006).
14. J. Nilsson, R. Paschotta, J. E. Caplen, and D. C. Hanna, "Yb3+-ring-doped fiber for high-energy pulse amplification," *Opt. Lett.* **22**(14), 1092–1094 (1997).
15. J. Nilsson, J. D. Minelly, R. Paschotta, A. C. Tropper, and D. C. Hanna, "Ring-doped cladding-pumped single-mode three-level fiber laser," *Opt. Lett.* **23**(5), 355–357 (1998).
16. R. S. Quimby, T. F. Morse, R. L. Shubochkin, and S. Ramachandran, "Yb3+ ring doping in high-order-mode fiber for high-power 977-nm lasers and amplifiers," *IEEE J. Sel. Top. Quantum Electron.* **15**(1), 12–18 (2009).
17. A. D. Yablon, "Recent progress in optical fiber refractive index profiling," presented at OFC/NFOEC 2011, March 6–10, Los Angeles, Paper No. OMF1 (2011).
18. N. M. Dragomir, G. W. Baxter, and A. Roberts, "Phase-sensitive imaging techniques applied to optical fibre characterization," *IEE Proc. Optoelectron.* **153**(5), 217–221 (2006).
19. F. El-Diasty, "Characterization of optical fibers by two- and multiple-beam interferometry," *Opt. Lasers Eng.* **46**(4), 291–305 (2008).
20. N. M. Dragomir, X. M. Goh, and A. Roberts, "Three-dimensional quantitative phase imaging: current and future perspectives," *Proc. SPIE* **6861**, 686106 (2008).
21. P. L. Chu and T. Whitbread, "Nondestructive determination of refractive index profile of an optical fiber: fast Fourier transform method," *Appl. Opt.* **18**(7), 1117–1122 (1979).
22. B. L. Bachim, T. K. Gaylord, and S. C. Mettler, "Refractive-index profiling of azimuthally asymmetric optical fibers by microinterferometric optical phase tomography," *Opt. Lett.* **30**(10), 1126–1128 (2005).
23. A. D. Yablon, "Measuring the spatial distribution of rare-earth dopants in high-power optical fibers," *Proc. SPIE* **7914**, 79141N (2011).
24. P. Chanclou, C. Kaczmarek, G. Mouzer, P. Gravey, M. Thual, M. A. Lecollinet, and P. Rochard, "Expanded single-mode fiber using graded index multimode fiber," *Opt. Eng.* **43**(7), 1634–1642 (2004).
25. A. D. Yablon, *Optical Fiber Fusion Splicing*, Springer (2005).
26. O. M. Sezerman, K. O. Hill, G. Best, D. R. J. Miller, M. Armstrong, and S. Lin, "Microstructuring optical wave guide devices with femtosecond optical pulses," U.S. Patent No. 7,095,931 (2006).
27. J. R. Marciante, "Gain Filtering for Single-Spatial-Mode Operation of Large-Mode-Area Fiber Amplifiers," *IEEE J. Sel. Top. Quant. Electron.* **15**(1), 30–36 (2009).
28. M. J. Söderlund, J. J. Montiel i Ponsoda, S. K. T. Tammela, K. Yla-Jarkko, A. Salokatve, and S. Honkanen, "Mode-induced transverse photodarkening loss variations in large-mode-area ytterbium doped silica fibers," *Opt. Exp.* **16**(14), 10633–10640 (2008).

Andrew D. Yablon earned his SB, SM, and PhD from MIT and is a founder and president of Interfiber Analysis, an optical fiber test and measurement company based in Livingston, New Jersey. He previously worked at Bell Laboratories in Murray Hill, New Jersey, OFS Laboratories in Somerset, New Jersey, and Vytran Corporation in Morganville, New Jersey. He is author of the monograph *Optical Fiber Fusion Splicing*, is listed as an author on about 30 peer-reviewed journal articles and about 50 conference publications, and holds 16 U.S. Patents. He served as chair of the Optical Fiber Subcommittee for OFC/NFOEC 2010, is a senior member of the OSA, and teaches the short course "Interconnection and fusion splicing of high-power optical fibers" at SPIE Photonics West.